Arch. Metall. Mater. **63** (2018), 3, 1477-1480

DOI: 10.24425/123833

D. PARK*[1], S.-J. OH*[1], I.-J. SHON*, S.-J. LEE*[#]

EFFECT OF Ni CONTENT ON THE AUSTENITE STABILITY AND MECHANICAL PROPERTIES OF NANOCRYSTALLINE Fe-Ni ALLOY FABRICATED BY SPARK PLASMA SINTERING

The mechanical behavior and the change of retained austenite of nanocrystalline Fe-Ni alloy have been investigated by considering the effect of various Ni addition amount. The nanocrystalline Fe-Ni alloy samples were rapidly fabricated by spark plasma sintering (SPS). The SPS is a well-known effective sintering process with an extremely short densification time not only to reach a theoretical density value but also to prevent a grain growth, which could result in a nanocrystalline structures. The effect of Ni addition on the compressive stress-strain behavior was analyzed. The variation of the volume fraction of retained austenite due to deformation was quantitatively measured by means of x-ray diffraction and microscope analyses. The strain-induced martensite transformation was observed in Fe-Ni alloy. The different amount of Ni influenced the rate of the strain-induced martensite transformation kinetics and resulted in the change of the work hardening during the compressive deformation.

Keywords: Fe-Ni alloy, austenite stability, mechanical properties, spark plasma sintering

1. Introduction

The control of austenite retained at room temperature is critically important to improve mechanical properties in Fe-based alloys. From the thermodynamic point of view, the austenite phase should be transformed to ferrite phase below the equilibrium A_{e1} temperature of about 727°C and no austenite can exist at room temperature in pure iron or Fe-based alloys. However, the austenite phase can be remained at room temperature by increasing the stability of austenite. The austenite stability can be increased by controlling the chemical composition of Fe-based alloy. The addition of austenite stabilizing elements such as Ni and Mn increases the austenite stability, resulting in the existence of metastable austenite retained at room temperature [1-3]. The grain refinement is very effective to increase the stability of austenite. Jimenez-Melero et al. [4] investigated the relationship between the grain size and the austenite stability in low-alloyed TRIP steels. Lee and coworkers [5] studied the effect of grain refinement on the martensite transformation kinetics related to austenite stability. The austenite phase can be stabilized mechanically. The presence of a sufficiently high dislocation density in austenite can effectively retard the kinetics of the martensite transformation [6].

Nickel is the most effective element to increase the austenite stability and a key alloying element to design various Fe-based austenitic alloys. Both the volume fraction and stability of metastable austenite retained at room temperature is controlled by Ni content in Fe-Ni alloys. Whereas no microstructural change during deformation at room temperature is observed in Fe-Ni alloy containing enough high Ni content, a metastable austenite is transformed mechanically during deformation in Fe-Ni alloy containing relatively low Ni content. This is known as the strain-induced martensite (SIM) transformation [7]. The formation of SIM from the austenite decomposition during deformation contributes the improvement of tensile strength, fatigue strength, and ductility [8,9].

The influence of Ni addition on the mechanical properties related to the SIM has been reported by several researchers [3,10], but there is an obvious limitation to reduce the grain size of austenite in order to maximize the austenite stability in conventional metallurgy processes including casting, forging/rolling, and heat treatment. Lee et al. [5] successfully produced ultrafine-grained medium Mn TRIP steel with an average grain size of 300 nm. However the reduction of the grain size below tens of nm through the conventional metallurgy processes is very difficult. Therefore, in the present study, we fabricated the nanocrystalline Fe-Ni alloy sample using spark plasma sintering (SPS) method. The SPS method can produce dense materials within a short process time which is very effective to prevent a grain growth. Some studies have reported about Fe-Ni alloys fabricated using SPS [11,12], but the previous works were focused on porosity effect, high-temperature oxidation, and so on. In the present study, we was mainly investigated the variation of the SIM transformation kinetics during deformation related to the austenite stability relying on the Ni content.

* CHONBUK NATIONAL UNIVERSITY, DIVISION OF ADVANCED MATERIALS ENGINEERING, 567 BAEKJE-DAERO, DEOKJIN-GU, JEONJU, 54896, REPUBLIC OF KOREA

[1] These authors equally contributed

Corresponding author: seokjaelee@jbnu.ac.kr

2. Experimental

The Fe powder with a purity of 99.9% and average particle size of <23.9 μm and Ni powder with a purity of 99.9% and average particle size of <7 μm were mixed to fabricate a nanocrystalline Fe-Ni alloy powder using a high-energy ball mill (a Pulverisette-5 planetary mill) at 250 rpm for 5 h under a pure Ar atmosphere. Tungsten carbide balls with diameters of 5 and 10 mm were used in a sealed cylindrical stainless steel jar with a ball to powder ratio of 30:1. The Ni content was varied from 11 to 15 wt.%. The milled Fe-Ni powder was filled in a cylindrical graphite die having an outer diameter of 35 mm, an inner diameter of 10 mm, and a height of 40 mm, which was sealed between upper and lower graphite punches. The SPS system was used. The milled Fe-Ni powder in a cylindrical graphite die was heated up to 1000°C with a heating rate of 1000°C/min and sintered at 1000°C for 1 minute under a high vacuum condition of below 150 mtorr. A uniaxial pressure of 80 MPa was mechanically applied during the sintering. The sintered sample was air-cooled to room temperature. Archimedes principle was adopted to measure the densities of sintered samples. The measured density of the sintered Fe-Ni alloy samples was almost identical to the theoretical density, which was higher than 98%. The theoretical densities were calculated to be 7.97, 7.99, and 8.02 cm^3/g for the Fe-11Ni, Fe-13Ni and Fe-15Ni, respectively. A cylindrical sample with a diameter of and a height of 4 mm was machined from the sintered sample for a compressive test. A room-temperature compressive test was carried out using a universal testing machine (Instron 8801) with a strain rate of 1×10^{-3} s^{-1}. The compressive test was stopped at a certain compressive strain in order to observe the microstructure change during deformation. The maximum compressive strain was 50%. Hardness measurements for the compressive test samples were performed using a Rockwell (HRC) hardness tester. A quantitative phase change was analyzed using X-ray diffraction (XRD) with a Cu Kα target at 40 kV and 30 mA (RIGAKU Max-2500). The samples were scanned from 30° to 100° of 2θ with a scan speed of 2°/min.

3. Results and discussion

Fig. 1 shows the plots of $B_r(= B_{crystalline} + B_{strain})\cos\theta$ versus $\sin\theta$ for calculating crystallite size of the milled Fe-Ni powders with different Ni content. The XRD patterns of the milled Fe-Ni powders was used with Suryanarayana and Grant Norton's formula [13]. The calculated crystallite sizes were 21, 15, and 19 nm for the Fe-11%Ni, Fe-13%Ni, and Fe-15%Ni, respectively. The Ni content barely affected the crystalline size. However, these crystallite size is remarkably small compared with the typical grain size of bulk Fe-based samples fabricated by conventional metallurgy processes.

Fig. 2 shows the XRD peaks of the sintered samples measured before and after the compressive test. The existence of the austenite peaks is observed regardless of Ni content in Fig. 2a. A minimum Ni content in order to remain austenite at room temperature is over 26 wt.% for the bulk Fe-Ni alloys [14]. However, the austenite peaks with intensities high enough as compared with ferrite peaks are also observed in the Fe-11%Ni sample. A considerable volume fraction of austenite retained at room temperature results from high stability of austenite due to the small crystallite size of about 20 nm. It is thought that nano-sized crystallite in the sintered Fe-Ni alloy can act as an actual grain size to increase the austenite stability effectively comparable to the grain refinement effect in the bulk Fe-Ni alloy. The peak intensities of austenite phase are gradually decreased as the compressive strain increases for all samples.

The decrease in the austenite peak intensity during deformation indicates the occurrence of SIM transformed from metastable austenite. The volume fraction change of austenite depending on compressive strain was calculated by XRD peak analysis using the following equation [15].

$$V_\gamma = \frac{\dfrac{I_{\gamma(200)} + I_{\gamma(220)} + I_{\gamma(311)}}{3}}{\dfrac{I_{\alpha(200)} + I_{\alpha(211)}}{2} + \dfrac{I_{\gamma(200)} + I_{\gamma(220)} + I_{\gamma(311)}}{3}} \quad (1)$$

where V_γ is the austenite volume fraction, I_γ and I_α are the peak intensity of austenite and ferrite, respectively. Fig. 3 compares the variation of the austenite volume fraction during the compressive test considering the Ni effect. The initial volume fractions of austenite before deformation were 48, 66, and 83 vol.% as increasing the Ni content. After the compressive deformation of 50%, the final volume fractions of austenite were 13, 21, and 33 vol.% for the Fe-11%Ni, Fe-13%Ni, and Fe-15%Ni, respectively. The decreased volume fraction of austenite indicates the volume fraction of SIM formed during deformation. The absolute

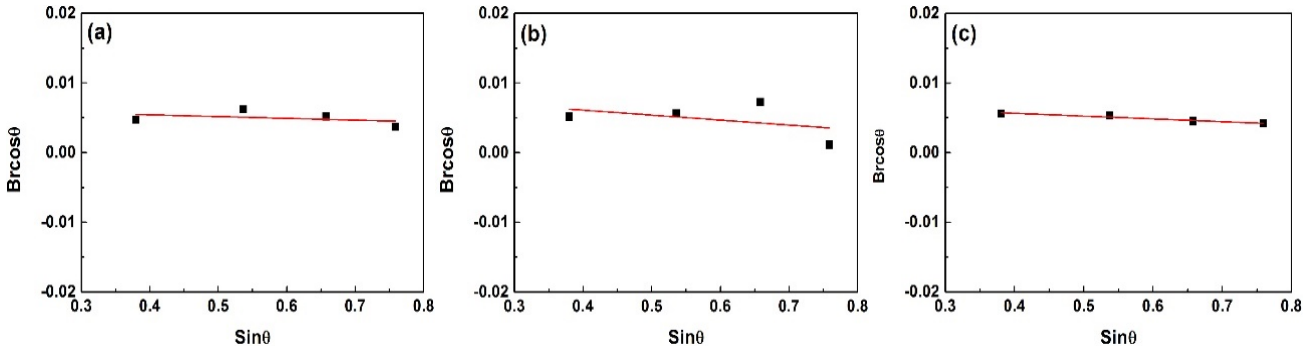

Fig. 1. Plot of $B_r\cos\theta$ versus $\sin\theta$ for the milled Fe-Ni powders: (a) Fe-11%Ni, (b) Fe-13%Ni, and (c) Fe-15%Ni

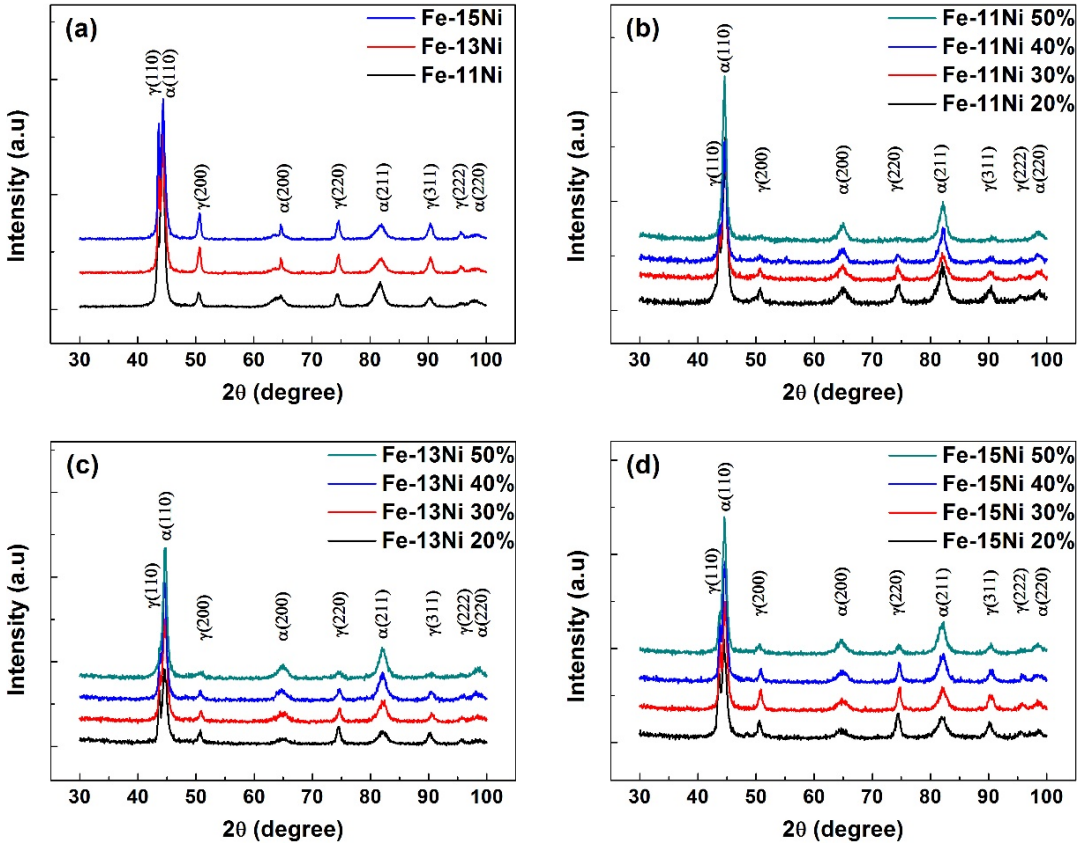

Fig. 2. XRD analyses of the sintered samples: (a) before compressive test, (b) deformed Fe-11%Ni, (c) deformed Fe-13%Ni, and (d) deformed Fe-15%Ni

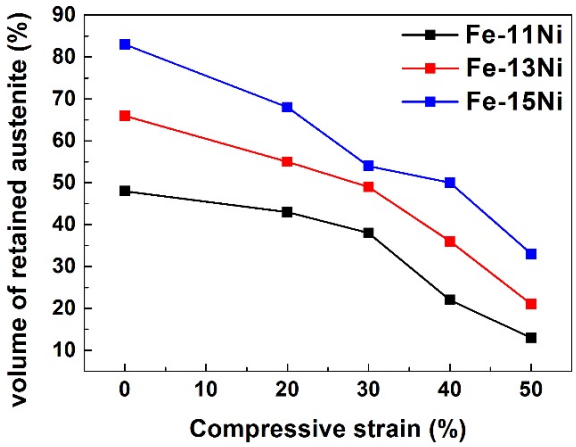

Fig. 3. Effect of Ni content on the variation of volume fraction of metastable austenite during compressive test

volume fraction of SIM in the Fe-15%Ni sample is higher than that in Fe-11%Ni or Fe-13%Ni samples. The relative ratio of the volume fraction of SIM to the volume fraction of the initial austenite before deformation is lowered as the Ni content increases from 0.729 to 0.602. This means that the austenite stability to prevent the decomposition of metastable austenite to martensite by deformation is also increased as increasing the Ni content.

Several models have been proposed to express the transformation kinetics of SIM as a function of strain. The model proposed by Burke [16], Matsumura et al. [17], Tsuchida and Tomota [18] was used to evaluate the transformation kinetics of SIM as follows:

$$V_{\alpha'} = \frac{V_\gamma^0}{1 + p/(k\varepsilon^p V_\gamma^0)} \tag{2}$$

where $V_{\alpha'}$ is the volume fraction of SIM, V_γ^0 is the initial volume fraction of austenite, and ε is the deformation strain. k is a constant related to the austenite stability. The k value is lowered as the stability of austenite increases. p is a constant concerning autocatalytic effect. It is reported that $p \approx 2$ for duplex stainless steel ($V_\gamma^0 \approx 0.5$) and $p \approx 3$ for metastable austenitic stainless steel ($V_\gamma^0 \approx 1$) [17]. The p value becomes one as the autocatalytic effect is negligible. Lee et al. [5] investigated that the nucleation rate for the martensite transformation of ultra-fine grained Fe-Mn-C alloys was accelerated as decreasing the grain size. In this study, the value of $p = 3$ was adopted.

Fig. 4 compares the SIM transformation kinetics predicted using Eq. (2) with the measured volume fractions depending on the Ni content. The predicted volume fraction changes show a good agreement with the measured results. The k values related to the austenite stability are 104.6, 69.7, and 52.9 for the Fe-11%Ni, Fe-13%Ni, and Fe-15%Ni, respectively. It means that the increase in Ni content increases the austenite stability, resulting in not only the higher volume fraction of austenite after the sintering but also the retarded transformation kinetics during deformation.

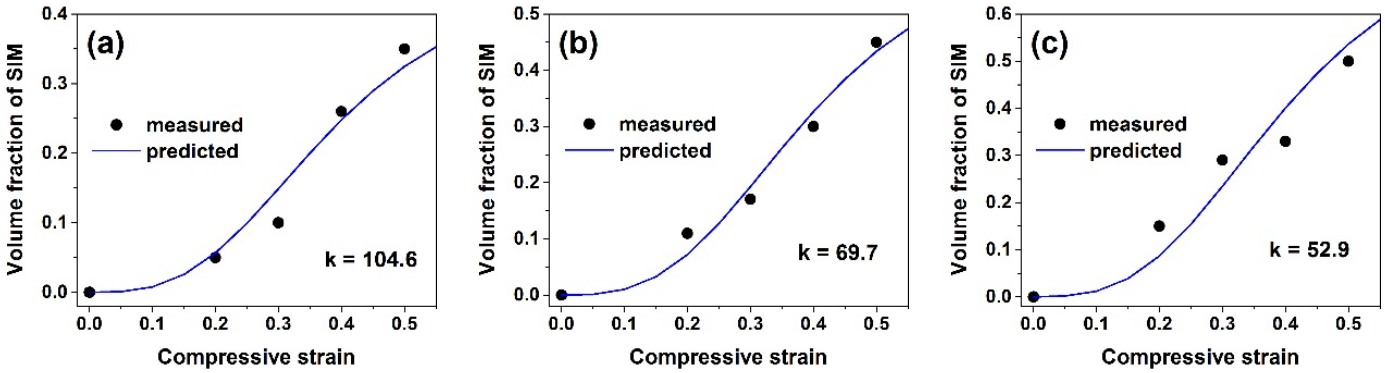

Fig. 4. Comparison of the SIM transformation kinetics depending on Ni content: (a) Fe-11%Ni, (b) Fe-13%Ni, and (c) Fe-15%Ni

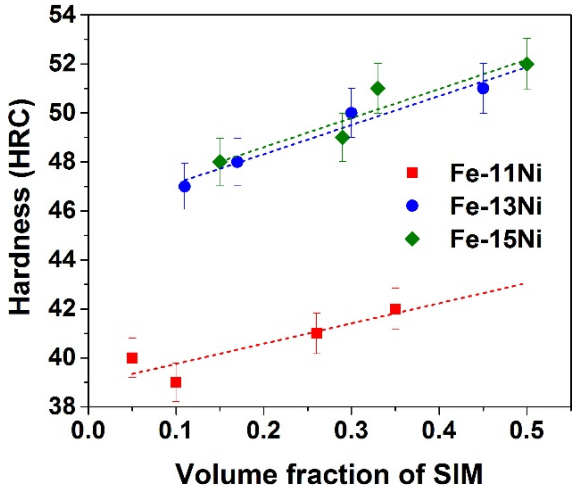

Fig. 5. Relationship between the volume fraction of SIM and the hardness value

Fig. 5 shows the hardness change according to the volume fraction change of SIM. The increase in hardness is almost linearly proportional to the increase in the volume fraction of SIM regardless of the Ni content. The higher the Ni content, the higher the hardness value. Actually, the Fe-15%Ni sample showed higher compressive yield and tensile strength than other two sample alloys due to the solid solution strengthening effect with more volume fraction of SIM formed during deformation.

4. Conclusions

In the present study, the Fe-Ni alloy samples with nano-sized crystallite were successfully fabricated by SPS method. A large volume fraction of austenite was remained at room temperature due to not only the addition of Ni but also the grain refinement effect. The variation of the volume fraction of austenite during compressive test was quantitatively analyzed by using the model considering the austenite stability factor *k*. The Ni content influenced the volume fraction of austenite and its stability, which affected not only the transformation kinetics of SIM during deformation but also influenced the hardness change of the sintered samples.

Acknowledgments

This research was supported by Basic Science Research Program through the National Research Foundation of Korea (NRF) funded by the Ministry of Education (2016R1D1A1B03935163).

REFERENCES

[1] S.J. Lee, S. Lee, B.C. De Cooman, Scripta Mater. **64**, 649 (2011).
[2] S. Lee, S.J. Lee, B.C. De Cooman, Scripta Mater. **65**, 225 (2011).
[3] K. Kim, S.J. Lee, Mater. Sci. Eng. A **698**, 183 (2017).
[4] E. Jimenez-Melero, N.H. Dijk, L. Zhao, J. Sietsma, S.E. Offerman, J.P. Wright, S. Zwaag., Scripta Mater. **56**, 421 (2007).
[5] S.J. Lee, S. Lee, B.C. De Cooman, Int. J. Mater. Res. **104**, 423 (2013).
[6] J. Mahieu, J. Maki, B.C. De Cooman, S. Claessens, Metall. Mater. Trans. A. **33A**, 2573 (2002).
[7] G.B. Olson, M. Cohen, Metall. Trans A **6**, 791 (1975).
[8] G.N. Haidemenopoulos, A.T. Kermanidis, C. Malliaros, H.H. Dickert, P. Kucharzyk, W. Bleck, Mater. Sci. Eng. A **573**, 7 (2013).
[9] A. Järvenpää, M. Jaskari, J. Man, L. Pentti Karjalainen, Mater. Charac. **127**, 12 (2017).
[10] S. Kim, C G. Lee, T.H. Lee, C.S. Oh, Scripta Mater. **48**, 539 (2003).
[11] M.B. Shongwe, S. Diouf, M.O. Durowoju, P.A. Olubambi, J. Alloys Compd. **649**, 824 (2015).
[12] C.H. Lim, J.S. Park, J.Y. Yun, J.K. Lee, J. Korean Powder Metall. Inst. **24**, 53 (2017).
[13] C. Suryanarayana, M. Grant Norton, X-ray diffraction A Practical Approach, Plenum Press, New York 1998.
[14] Y. Huizhou, M. Harmelin, J. Bigot, Mater. Sci. Eng. A **124**, 241 (1990).
[15] ASTM E975-00, Standard Practice for X-Ray Determination of Retained Austenite in Steel with Near Random Crystallographic Orientation, vol. 03. 01, ASTM International, W. Conshohocken, PA, 2003.
[16] J. Burke, Kinetics of Phase Transformation in Metals, Pergamon Press, Oxford, United Kingdom, 1965.
[17] O. Matsumura, Y. Sakuma, H. Takechi, Scripta Metall. **21**, 1301 (1987).
[18] N. Tsuchida, Y. Tomota, Mater. Sci. Eng. A **285**, 345 (2000).